Abdominal Radiology

Published online: 31 July 2018

Abdom Radiol (2019) 44:279–285
https://doi.org/10.1007/s00261-018-1718-6

Predictive role of PI-RADSv2 and ADC parameters in differentiating Gleason pattern 3 + 4 and 4 + 3 prostate cancer

Francesco Alessandrino,[1,2] Mehdi Taghipour,[1] Elmira Hassanzadeh,[1,3] Alireza Ziaei,[1] Mark Vangel,[1] Andriy Fedorov,[1] Clare M. Tempany,[1] and Fiona M. Fennessy[1,2]

[1]Department of Radiology, Brigham and Women's Hospital, Harvard Medical School, 75 Francis Street, Boston, MA 02215, USA
[2]Department of Imaging, Dana Farber Cancer Institute, Harvard Medical School, Boston, MA, USA
[3]Department of Radiology, University of Illinois at Chicago, Chicago, IL, USA

Abstract

Purpose: To compare the predictive roles of qualitative (PI-RADSv2) and quantitative assessment (ADC metrics), in differentiating Gleason pattern (GP) 3 + 4 from the more aggressive GP 4 + 3 prostate cancer (PCa) using radical prostatectomy (RP) specimen as the reference standard.
Methods: We retrospectively identified treatment-naïve peripheral (PZ) and transitional zone (TZ) Gleason Score 7 PCa patients who underwent multiparametric 3T prostate MRI (DWI with *b* value of 0,1400 and where unavailable, 0,500) and subsequent RP from 2011 to 2015. For each lesion identified on MRI, a PI-RADSv2 score was assigned by a radiologist blinded to pathology data. A PI-RADSv2 score ≤ 3 was defined as "low risk," a PI-RADSv2 score ≥ 4 as "high risk" for clinically significant PCa. Mean tumor ADC (ADC_T), ADC of adjacent normal tissue (ADC_N), and ADC_{ratio} (ADC_T/ADC_N) were calculated. Stepwise regression analysis using tumor location, ADC_T and ADC_{ratio}, *b* value, low vs. high PI-RADSv2 score was performed to differentiate GP 3 + 4 from 4 + 3.
Results: 119 out of 645 cases initially identified met eligibility requirements. 76 lesions were GP 3 + 4, 43 were 4 + 3. ADC_{ratio} was significantly different between the two GP groups ($p = 0.001$). PI-RADSv2 score ("low" vs. "high") was not significantly different between the two GP groups ($p = 0.17$). Regression analysis selected ADC_T ($p = 0.03$) and ADC_{ratio} ($p = 0.0007$) as best predictors to differentiate GP 4 + 3 from 3 + 4. Estimated sensitivity, specificity, and accuracy of the predictive model in differentiating GP 4 + 3 from 3 + 4 were 37, 82, and 66%, respectively.
Conclusions: ADC metrics could differentiate GP 3 + 4 from 4 + 3 PCa with high specificity and moderate accuracy while PI-RADSv2, did not differentiate between these patterns.

Key words: Prostate cancer—Magnetic resonance imaging—Diffusion-weighted imaging—Apparent diffusion coefficient—PI-RADSv2—Gleason score

Prostate cancer (PCa), one of the most common malignancies in adult men, represents a heterogeneous disease, with 5-year survival ranging from 100% for localized disease to 29% in patients with metastatic PCa [1]. The Gleason Score (GS), implemented in 1974, has served as a strong predictor of outcome for localized disease [2–4]. Nonetheless, for PCa with GS = 7 on radical prostatectomy (RP) recurrence rate varies considerably, depending also on primary Gleason Pattern (GP), with 5-year biochemical risk-free survival of 88% for GP 3 + 4 but only 63% for 4 + 3 PCa [5]. There also has been reported a three-fold increase in mortality for GP 4 + 3 PCa compared to GP 3 + 4 PCa [6, 7]. To reflect these differences, in 2014, the International Society of Urological Pathology Consensus Conference proposed a new PCa histological Grading System, differentiating GS = 7 PCa into either Grade Group 2 (GP 3 + 4) or Grade Group 3 (GP 4 + 3) [8].

Prostate multiparametric MRI (mpMRI) has emerged as a valuable tool for detection and localization of PCa, for treatment guidance, and for PCa risk strat-

Correspondence to: Francesco Alessandrino; *email:* falessandrino@bwh.harvard.edu

ification [9, 10]. Acquisition of apparent diffusion coefficient (ADC) maps, derived from diffusion-weighted imaging (DWI), is recommended by the American College of Radiology as part of standardized mpMRI protocol, as it has been shown that adding DWI and ADC maps increases accuracy for PCa detection and localization [11, 12]. Quantitative metrics derived from ADC, including mean, median ADC, and ADC ratio (defined as the ratio of ADC values of tumor to normal tissue) have been shown to inversely correlate with GS, confirmed on RP specimens [13–15]. Among the various metrics, ADC ratio has been shown to correlate best with GS on RP [14, 16]. ADC ratio is also thought to overcome the variability of absolute ADC values related to both patient and technical factors (such as DWI *b* value) [16–18] In the heterogeneous GS = 7 PCa group, ADC metrics have been shown to be helpful in differentiating GP 3 + 4 from GP 4 + 3 PCa, with mean ADC and ADC entropy (a textural-based measure of the variation of the ADC values across the lesion) helpful in differentiating between these 2 patterns [19, 20].

The Prostate Imaging Reporting and Data System version 2 (PI-RADS v2) is a qualitative MRI-based reporting system, which was first introduced 2012 by the European Society of Urogenital Radiology, and updated to its second version by a larger international group, whose aim is to standardize mpMRI acquisition, interpretation, and reporting [12, 21]. PI-RADSv2 utilizes a 5-point scale to determine the likelihood of clinically significant PCa, and is based upon qualitative interpretation of DWI/ADC, dynamic contrast-enhanced MRI (DCE-MRI), and T2-weighted imaging (T2WI) [12]. PI-RADSv2 has shown to improve preoperative detection of clinically significant PCa, but there is scarce data regarding its predictive role in discriminating GP 3 + 4 from GP 4 + 3 PCa [12, 22].

The aim of this study was to evaluate the predictive roles of qualitative PI-RADSv2 and quantitative ADC metrics (mean ADC and ADC ratio) in differentiating GP 3 + 4 PCa from the more aggressive 4 + 3 PCa, as defined on RP.

Materials and methods

Patients

This retrospective study was HIPAA compliant and approved by the local Institutional Review Board. Using our institutional search engine, we first queried cases with diagnosis of prostate cancer; who underwent multiparametric 3T prostate mpMRI from 2011 to 2015; and with history of RP. Of the retrieved cases, only treatment-naive GS = 7 either in the peripheral (PZ) or transitional zone (TZ) PCa cases were included in the study.

MRI technique

All MRI examinations were performed on a 3.0 T magnet (GE Signa HDx, GE Healthcare, Waukesha, WI) using an eight-channel abdominal array and endorectal coil (Medrad, Pittsburgh, PA), as previously described [23, 24]. Our protocol included spoiled gradient echo (SPGR) T1-weighted sequences with repetition time (TR)/echo time (TE)/α = 385 ms/6.2 ms/65°, over a 16-cm^2 field of view (FOV); fast relaxation fast spin echo (FRFSE) T2-weighted sequences with TR/TE = 3500 ms/102 ms over a 16-cm^2 FOV; single-shot echo planar (EPI) DWI sequences with TR/TE = 2500 ms/65 ms and TR/TE = 3000 ms/80 ms for 0,500 0,1400 s/mm^2 *b* values, respectively. In addition, 3D SPGR DCE sequences were acquired with TR/TE/α = 3.6 ms/1.3 ms/15°, with full-gland coverage, and image voxel size of 1 × 1 × 6 mm^3, as previously described [25]. Temporal resolution was 5 s, for a total observation time of 5 min Gadopentetate dimeglumine (Magnevist, Berlex Laboratories, Wayne, NJ) was injected intravenously (0.15 mmol/kg) at 3 mL/s injection rate.

Clinical and histopathologic information collection

Subjects' age, serum prostate-specific antigen (PSA) at the time of diagnosis, date of prostate mpMRI, and date of RP were collected using our electronic medical records database. The histopathology reports of the RP specimens were reviewed, and primary and secondary GP were recorded. All RP specimens were processed according to the Stanford protocol [26, 27].

Image analysis

A single radiologist (F.F.), with over 15 years of experience interpreting prostate MRI, reviewed the de-identified mpMRIs to identify the index lesion. The radiologist was aware of a diagnosis of PCa, age, and PSA levels, but was blinded to GS and GP. Tumor location (PZ or TZ) and highest DWI *b* value (500 or 1400 s/mm^2) were recorded. An overall PI-RADSv2 assessment score (based upon T2, DWI/ADC, and DCE) was assigned using PI-RADSv2 recommended algorithm (12). A PI-RADSv2 score of 4 or 5 was defined as "high risk," whereas a PI-RADSv2 score ≤ 3 was defined as "low risk."

All available MRI images for each case were viewed to identify the index tumor (T). After T was identified, Circular regions of interest (ROI) were drawn on ADC maps (b = 0,500, or b = 0,1400) on the index tumor (T), encompassing most of the lesion, and on the normal (N) prostatic tissue (an area of noncancerous tissue similar in size and in the same prostate zone of the T). T2-weighted, DCE, and DWI images were used as a reference when the index lesion was not visible on ADC maps. Mean ADC for T (ADC_T) and N (ADC_N) were calculated for each ROI. ADC_{ratio} was defined as ADC_T/ADC_N.

Statistical analysis

Continuous variables were summarized using means and ranges, and categorical variables were summarized using frequencies and percentages. Independent sample t test, or Mann–Whitney test when data were not normally distributed, was used to compare ADC_T and ADC_{ratio} in the two groups (GP 3 + 4 vs. 4 + 3). Comparison between location on MRI (PZ vs. TZ), DWI *b* value (500 vs. 1400 s/mm^2), and PI-RADSv2 score was carried out with a χ^2 or Fisher's exact test in the two groups. Stepwise logistic regression analysis using location on MRI (PZ and TZ), ADC_T, ADC_{ratio}, *b* value (either 500 or 1400), and PI-RADSv2 score as predictors and GP 4 + 3 as response was performed. A two-tailed p value less than 0.05 was considered significant. All statistical analyses were performed using STATA (Version 11.2 StataCorp College Station, Texas USA).

Results

Patients and tumor characteristics

A total of 645 patients who had a prostate mpMRI and RP-confirmed PCa were identified from the initial query. We excluded patients who did not have an RP within a 6-month window of the mpMRI ($n = 434$), those with a GS ≤ 6 or ≥ 8 ($n = 78$), and those with no identifiable lesion on mpMRI ($n = 9$). 124 patients were initially retrieved. Those with diffuse PCa lesions encompassing the PZ and TZ ($n = 1$), lesions located in the central zone ($n = 3$) or in the anterior fibromuscular stroma ($n = 1$) were excluded. Our final population consisted of 119 patients with a PZ- or TZ-dominant lesion (Figs. 1, 2).

Tumor characteristics are reported in Table 1. Of the 119 lesions, 76 lesions were GP 3 + 4 and 43 were GP 4 + 3. Mean age was 59.48 years (range 43–76 years) and mean PSA was 7.29 ng/ml (range 1.64–38.7).

MRI analysis

MRI characteristics of the included cases are also reported in Table 1. Of the 119 identifiable PCa lesions, 99 were located in the PZ and 20 were located in the TZ. Tumor location on MRI (PZ vs. TZ) did not differ between the two GP groups ($p = 0.693$).

ADC and b value

Fifty-one mpMRIs were performed with highest DWI *b* value of 500 s/mm^2, 68 were performed with highest DWI *b* value of 1400 s/mm^2. The proportion of mpMRI performed with different *b* values utilized for ADC analysis (500 vs. 1400) did not differ between the two GP groups ($p = 0.321417$). Median ADC_T was 823 [lower quartile (Q1)–upper quartile (Q3): 698.25–987.5] and 717 [Q1–Q3: 632–1004], and median ADC_{ratio} was 0.6103 [Q1–Q3: 0.538–0.746] and 0.5346 [Q1–Q3: 0.466–0.607] for GS 3 + 4 and 4 + 3, respectively. ADC_T did not significantly differ between the two GP groups ($p = 0.1936$). ADC_{ratio} was significantly different between the two GP groups ($p = 0.001$).

PI-RADSv2

A total of 110 lesions were categorized as "high" PI-RADSv2 score (PI-RADSv2 score ≥ 4). Of these, 68 lesions were PI-RADSv2 score 4 and 32 were PAC 5. Regarding tumor location, 60 PZ lesions were categorized as PI-RADSv2 score 4 and 32 PZ lesions were PAC 5, whereas 8 TZ lesions were categorized as PI-RADSv2 score 4 and 10 were categorized as PI-RADSv2 score 5. Regarding GP groups, 46 3 + 4 GP lesions were PI-RADSv2 score 4, 22 were PI-RADSv2 score 5, whereas 23 4 + 3 GP lesions were PI-RADSv2 score 4, and 19 were PI-RADSv2 score 5. There was no significant association between "high" PI-RADSv2 score and 4 + 3 PCa (0.485). When only "high" PI-RADSv2 score lesions were considered, no significant difference between PI-RADSv2 score 4 or 5 assigned between the two GP groups was observed ($p = 0.174$).

Logistic regression analysis and predictive model

Logistic regression was performed with GP = 4 + 3 as response, and location, ADC_T and ADC_{ratio}, *b* value, and PI-RADSv2 score as predictors. Cases with PI-RADSv2 score < 4 were excluded from analysis, and a total of 110 cases were included in the model. A stepwise regression starting with the full model and minimizing AIC (Akaike Information Criterion) resulted in the selection of a model which included only ADC_T and ADC_{ratio} ($p = 0.04$ and 0.002, respectively, AIC = 139.1). Thresholding the fitted values from this regression at 0.5, the estimated sensitivity of the predictive model in differentiating GP 4 + 3 from 3 + 4 PCa was 37%, specificity 83%, and accuracy 65%. Including 5 PI-RADSv2 score = 3 cases did not significantly change the results, and only ADC_T and ADC_{ratio} were selected in the model ($p = 0.03$ and 0.0007, respectively, AIC = 149). Estimated sensitivity of the model was 40%, specificity 82%, and accuracy 67%. When all 119 cases were included, only ADC_T and ADC_{ratio} were selected ($p = 0.0359$ and 0.0004, respectively) resulting in a model with estimated sensitivity of 37%, specificity of 82%, and accuracy of 65%.

Discussion

Gleason 7 PCa represents a heterogeneous population of PCa comprising GP 3 + 4 and GP 4 + 3 lesions with different recurrence rate, prognosis, and treatment [7]. In this study, we showed that quantitative ADC_T and

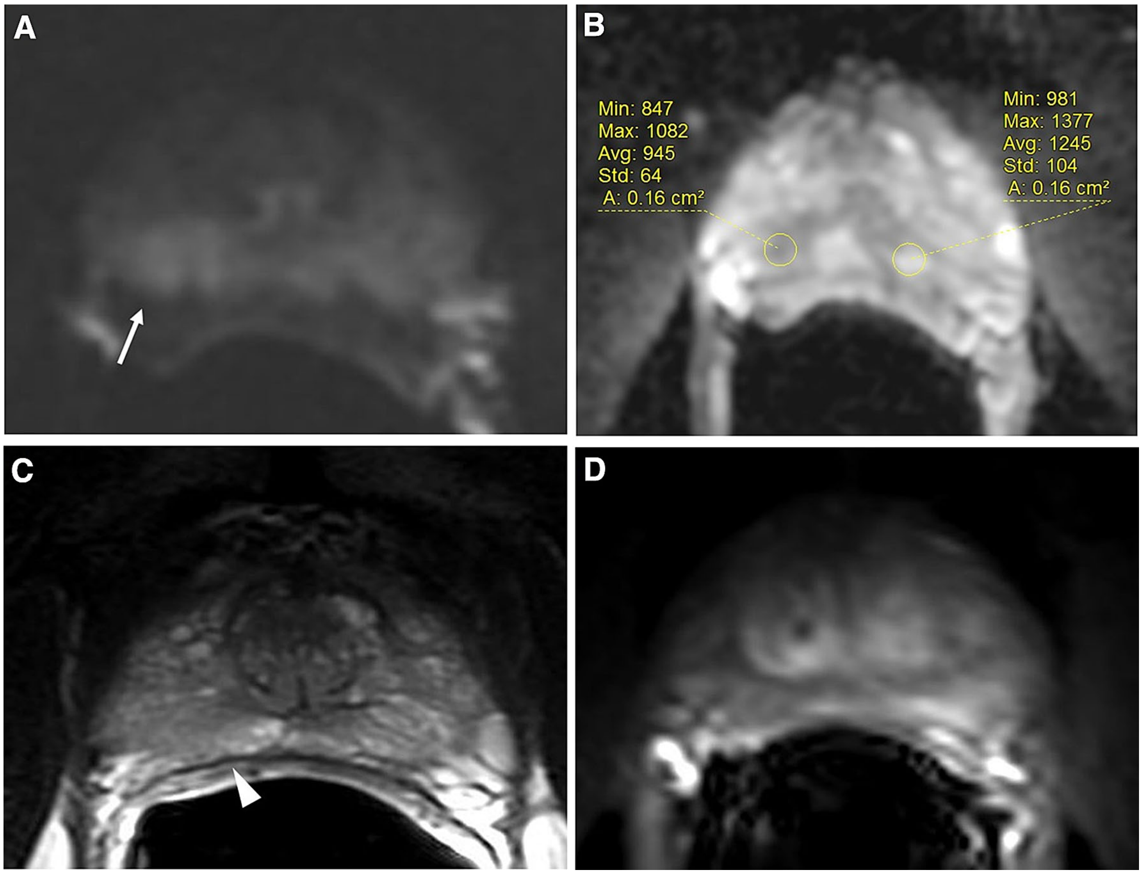

Fig. 1. A 52-year-old man with Gleason pattern 3 + 4 peripheral zone prostate cancer. **A** Diffusion-weighted image (DWI) performed with *b* value of 1400 mm/s^2 shows a diffusion restricting lesion in the right peripheral zone (white arrow), markedly hypointense on attenuation diffusion coefficient (ADC) map, corresponding to a DWI score of 4 according to PI-RADS v2 (**B**). **C** T2-weighted (T2 W) image shows a corresponding heterogeneous moderately hypointense non-circumscribed lesion, measured < 1.5 cm in greatest dimension confined to prostate (white arrowhead), corresponding to a T2 W score of 3 according to PI-RADS v2. Dynamic contrast-enhanced (DCE) image showed no corresponding focal or early enhancement, and a negative DCE score was assigned (**D**). A PI-RADS v2 score of 4 was assigned to the lesion. The mean ADC mean of the lesion was 945 and the ADC ratio was 0.76 (**B**).

ADC_{ratio} predict differentiation between GP 3 + 4 and 4 + 3 PCa, with an accuracy of 67%. In our population, we could not demonstrate a role for PI-RADSv2 in predicting GS = 7 PCa subtype. In addition, we demonstrated that ADC_{ratio} was significantly different between the two GP 3 + 4 and 4 + 3 PCa, whereas no significant difference in the ADC_T was observed between the two groups.

The role of ADC metrics in differentiating GP 3 + 4 vs. 4 + 3 PCa has been addressed by few studies [19, 20, 28]. A study on 57 GS = 7 PCa showed that ADC/T2 ratio, defined as the ratio of ADC values and of the signal intensity of the tumor measured, respectively, on ADC maps and T2WI, had a sensitivity of 77.5% and a specificity of 64.7% in discriminating GP 3 + 4 from 4 + 3 PCa [29]. In our study, a predictive model comprising only ADC_T and ADC_{ratio} to differentiate GP 4 + 3 from 3 + 4 PCa, showed sensitivity of 37%, specificity of 83%, and accuracy 65%, when cases with PI-RADSv2 score ≥ 4 were included. Our comparatively low sensitivity may be explained by the fact that our population was composed solely of GS = 7, and differentiation between GP 3 + 4 and 4 + 3 may be more challenging that differentiation of GS = 7 from GS 6 or 8.

We found that ADC_T was not significantly different between GP 3 + 4 and GP 4 + 3 PCa. These findings are discordant with a study that correlated ADC and GP [20]. In this study of 37 patients with GS = 7 PCa, mean ADC was significantly different between GP 3 + 4 and GP 4 + 3 [20]. In the study by Itou et al., all cases were obtained with *b* values of 0,1000 s/mm^2, and absolute ADC values, including mean ADC_T, are dependent on the *b* value selected [17, 20]. It is possible that the difference might be explained by the different *b* values used in the two studies, as ADC was obtained in 51 of our cases using *b* values of 0,500 s/mm^2 and using 0,1400 s/mm^2 in 68 cases. Interestingly, a more recent study on 84

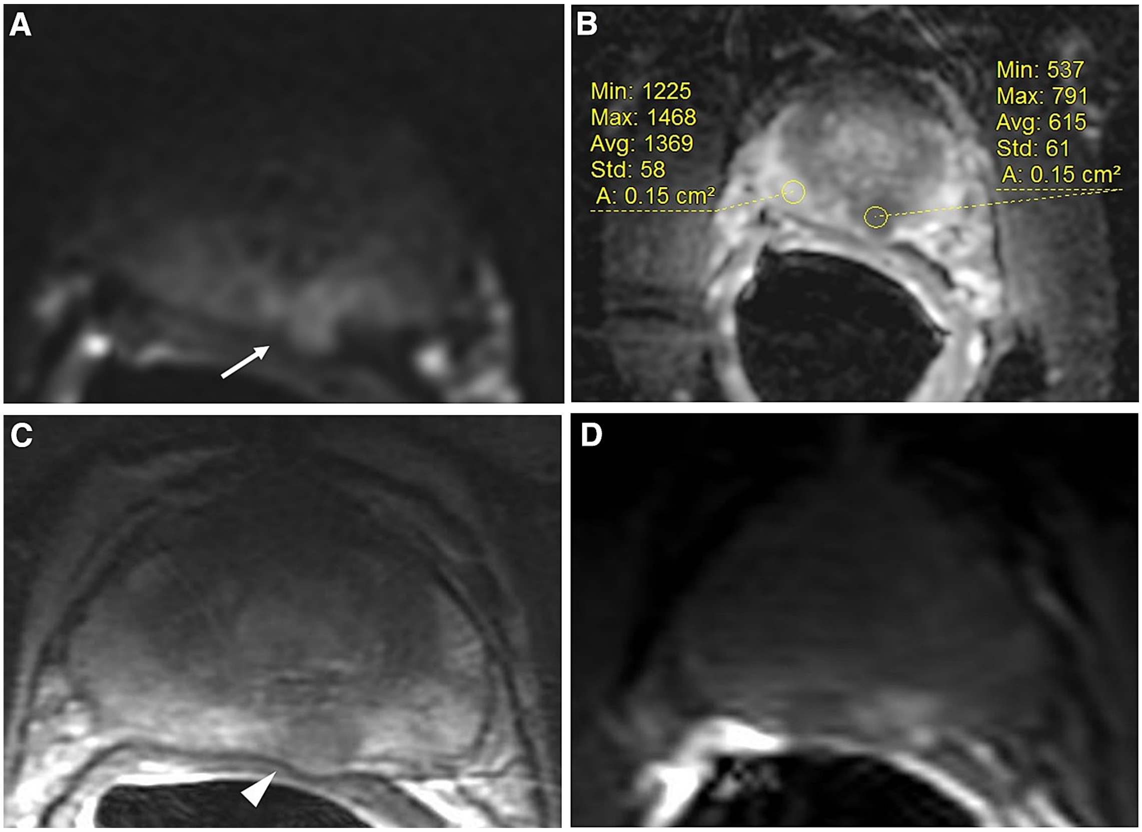

Fig. 2. A 68-year-old man with Gleason pattern 4 + 3 peripheral zone prostate cancer. **A** Diffusion-weighted image (DWI) performed with b value of 1400 mm/s^2 shows a diffusion restricting lesion in the left peripheral zone (white arrow), markedly hypointense on attenuation diffusion coefficient (ADC) map, corresponding to a DWI score of 4 according to PI-RADS v2 (**B**). **C** T2-weighted (T2 W) image shows a corresponding round hypointense area, measured < 1.5 cm in greatest dimension confined to prostate (white arrowhead), corresponding to a T2 W score of 4 according to PI-RADS v2. Dynamic contrast-enhanced (DCE) image showed corresponding focal early enhancement, and a positive DCE score was assigned (**D**). A PI-RADS v2 score of 4 was assigned to the lesion. The mean ADC of the lesion was 615 and the ADC ratio was 0.45 (**B**).

GS = 7 PCa showed no significant difference in mean ADC of GP 3 + 4 vs. 4 + 3 Pca [19]. Another study evaluated mean ADC in 21 GS = 7 PCa, showing no significant difference the two GP groups [29].

Regarding ADC_{ratio}, various studies have addressed the role of this ADC metric in differentiating PCa with different GS [14, 16]. A recent study on 45 PCa patient, 21 of which were GS = 7, showed significant difference in ADC_{ratio} in differentiating GP 3 + 4 and 4 + 3 lesions [29]. De Cobelli et al., showed that ADC_{ratio} could differentiate between GS 6, 7, and 8-10 PCa; however, no data regarding differentiation between different GP 3 + 4 and 4 + 3 PCa were presented [14]. Woo et al. evaluated the role of various ADC_{ratio} in differentiating GS = 6 from GS ≥ 7 PCa, yet no data regarding the predictive role of ADC_{ratio} in differentiating GP 3 + 4 and 4 + 3 lesions were reported [14, 16].

Our results, showing that only ADC_{ratio} was significantly different between GP 3 + 4 and 4 + 3 PCa, reflect the data reported in literature, as few studies comparing ADC and ADC_{ratio} found that the latter was superior to mean ADC in determining aggressive PCa, including a study on 21 GS 7 PCa patients who showed that ADC_{ratio} was significantly different, while mean ADC was not significantly different [15, 29–31]. Nonetheless other data suggest similar performance of mean ADC and ADC_{ratio} in determining aggressive PCa [14]. Our results may be explained by the fact that ADC_{ratio} is relatively independent of the *b* value used, whereas absolute ADC values depend on the *b* value selected [17].

Regarding the predictive role of PI-RADSv2, we found no role for PI-RADSv2 in differentiating GP 3 + 4 vs. 4 + 3 PCa. In addition, no association between GP and PAC was observed. A prior study on 425 PCa evaluated the role of PI-RADS to predict clinically significant PCa [22]. Although 250 GS = 7 PCa cases were included in the analysis, no analysis of the role of

Table 1. Tumor and MRI characteristics (GS, location, ADC, PI-RADSv2 score)

	Gleason pattern		p value
	3 + 4	4 + 3	
Location			
PZ	64	35	0.693
TZ	12	8	
b value DWI			
0,500	30	15	0.321
0,1400	46	28	
ADC [median; Q1–Q3]			
ADC_T	823 [698.25–987.5]	717 [632–1004]	0.1936
ADC_{ratio}	0.6103 [0.538–0.746]	0.5346 [0.466–0.607]	**0.001**
PI-RADSv2 score			
2	3	1	0.485*
3	4	1	
4	46	22	
5	23	19	
Total	76	43	

Clinically significant value is highlighted in bold
PZ, peripheral zone; TZ, transitional zone; DWI, Diffusion-weighted imaging; ADC, apparent diffusion coefficient; Q1, lower quartile; Q3, upper quartile
*Association between PI-RADSv2 score ≥ 4 and Gleason Pattern 4 + 3

PI-RADSv2 in differentiating GP 3 + 4 vs. 4 + 3 PCa was performed [22].

Our study has several limitations. First, it is a retrospective study. Although the radiologist was blinded to the GS, the evaluation of a predictive role of a diagnostic test is inherently limited, given the study type. In addition, retrospective studies rely on others for accurate recordkeeping and some biases such as selection bias and misclassification or information bias can negatively impact the veracity of this type of study. Furthermore, we used different b values for DWI, and not all cases were performed with b value of 1400 s/mm^2. Specifically, more than one-third of mpMRI, performed before PI-RADSv2 recommendation for the use of high b value was available, had highest b value of 500 s/mm^2 [12]. Although both GP groups had the same proportion of mpMRI performed with low b value, this might have reduced the performance of ADC_T and the diagnostic performance of PI-RADSv2 [12, 32]. Nonetheless, various studies showed that mean ADC was significantly different for GP ≤ 3 + 4 vs. GP ≥ 4 + 3 PCa, even when acquired on DWI with b values < 1000 mm/s^2 [33–35]. Lastly, mpMRI were analyzed by a single reader, who however had over 15 years of experience in interpreting prostate MRI. Inter-reader agreement was not evaluated. However, a recent study evaluated inter-reader agreement of PI-RADS v2 for detection of GP ≥ 3 + 4 PZ PCa, showing almost perfect agreement ($k > 0.9$) [36].

In conclusion, our findings suggest that quantitative ADC metrics can predict differentiation between GP 3 + 4 and 4 + 3 PCa, with acceptable accuracy, whereas PI-RADSv2 did not have a predictive role.

Compliance with ethical standards

Funding National Institute of Health—National Cancer Institute: U01 CA151261; R25 CA089017; NIH P41EB 015898.

Conflict of interest Francesco Alessandrino, Mehdi Taghipour, Elmira Hassanzadeh, Alireza Ziaei, and Mark Vangel declare they have no conflict of interest. Andriy Fedorov received the following grants from Institute of Health—National Cancer Institute: U01 CA151261; NIH P41EB 015898. Clare M Tempany received the following grants from Institute of Health—National Cancer Institute: R25 CA089017; NIH P41EB 015898. Fiona M Fennessy received the following grants from Institute of Health—National Cancer Institute: U01 CA151261; R25 CA089017; NIH P41EB 015898.

Ethical approval All procedures performed in studies involving human participants were in accordance with the ethical standards of the institutional and/or national research committee and with the 1964 Helsinki declaration and its later amendments or comparable ethical standards.

Informed consent For this type of study formal consent is not required.

References

1. Siegel RL, Miller KD, Jemal A (2017) Cancer statistics, 2017. CA Cancer J Clin 67(1):7–30
2. Quinn DI, Henshall SM, Haynes AM, et al. (2001) Prognostic significance of pathologic features in localized prostate cancer treated with radical prostatectomy: implications for staging systems and predictive models. J Clin Oncol 19(16):3692–3705
3. Gleason DF, Mellinger GT (1974) Prediction of prognosis for prostatic adenocarcinoma by combined histological grading and clinical staging. J Urol 111(1):58–64
4. Andrén O, Fall K, Franzén L, et al. (2006) How well does the Gleason score predict prostate cancer death? A 20-year followup of a population based cohort in Sweden. J Urol 175(4):1337–1340
5. Stark JR, Perner S, Stampfer MJ, et al. (2009) Gleason score and lethal prostate cancer: does 3 + 4 = 4 + 3? J Clin Oncol 27(21):3459–3464
6. Epstein JI, Zelefsky MJ, Sjoberg DD, et al. (2016) A contemporary prostate cancer grading system: a validated alternative to the Gleason score. Eur Urol 69(3):428–435
7. Kane CJ, Eggener SE, Shindel AW, Andriole GL (2017) Variability in outcomes for patients with intermediate-risk prostate cancer (Gleason Score 7, International Society of Urological Pathology Gleason Group 2–3) and implications for risk stratification: a systematic review. Eur Urol Focus 3(4–5):487–497
8. Epstein JI, Egevad L, Amin MB, Delahunt B, Srigley JR, Humphrey PA; Grading Committee (2016) The 2014 International Society of Urological Pathology (ISUP) consensus conference on gleason grading of prostatic carcinoma: definition of grading patterns and proposal for a new grading system. Am J Surg Pathol 40(2):244–252
9. Hoeks CMA, Barentsz JO, Hambrock T, et al. (2011) Prostate cancer: multiparametric MR imaging for detection, localization, and staging. Radiology 261(1):46–66
10. Jambor I, Boström PJ, Taimen P, et al. (2017) Novel biparametric MRI and targeted biopsy improves risk stratification in men with a clinical suspicion of prostate cancer (IMPROD Trial). J Magn Reson Imaging 46(4):1089–1095
11. Wu L-M, Xu J-R, Ye Y-Q, Lu Q, Hu J-N (2012) The clinical value of diffusion-weighted imaging in combination with T2-weighted imaging in diagnosing prostate carcinoma: a systematic review and meta-analysis. AJR 199(1):103–110
12. Weinreb JC, Barentsz JO, Choyke PL, et al. (2016) PI-RADS prostate imaging—reporting and data system: 2015, Version 2. Eur Urol 69(1):16–40
13. Hambrock T, Somford DM, Huisman HJ, et al. (2011) Relationship between apparent diffusion coefficients at 3.0-T MR imaging and Gleason grade in peripheral zone prostate cancer. Radiology 259(2):453–461

14. De Cobelli F, Ravelli S, Esposito A, et al. (2015) Apparent diffusion coefficient value and ratio as noninvasive potential biomarkers to predict prostate cancer grading: comparison with prostate biopsy and radical prostatectomy specimen. AJR 204(3):550–557
15. Woo S, Kim SY, Cho JY, Kim SH (2016) Preoperative evaluation of prostate cancer aggressiveness: using ADC and ADC ratio in determining gleason score. AJR 207(1):114–120
16. Barrett T, Priest AN, Lawrence EM, et al. (2015) Ratio of tumor to normal prostate tissue apparent diffusion coefficient as a method for quantifying DWI of the prostate. AJR 205(6):W585–593
17. Litjens GJS, Hambrock T, Hulsbergen-van de Kaa C, Barentsz JO, Huisman HJ (2012) Interpatient variation in normal peripheral zone apparent diffusion coefficient: effect on the prediction of prostate cancer aggressiveness. Radiology 265(1):260–266
18. Peng Y, Jiang Y, Antic T, et al. (2014) Apparent diffusion coefficient for prostate cancer imaging: impact of b values. AJR 202(3):W247–253
19. Rosenkrantz AB, Triolo MJ, Melamed J, et al. (2014) Whole-lesion apparent diffusion coefficient metrics as a marker of percentage Gleason 4 component within Gleason 7 prostate cancer at radical prostatectomy. J Magn Reson Imaging 41(3):708–714
20. Itou Y, Nakanishi K, Narumi Y, Nishizawa Y, Tsukuma H (2011) Clinical utility of apparent diffusion coefficient (ADC) values in patients with prostate cancer: can ADC values contribute to assess the aggressiveness of prostate cancer? J Magn Reson Imaging 33(1):167–172
21. Barentsz JO, Richenberg J, Clements R, et al. (2012) ESUR prostate MR guidelines 2012. Eur Radiol 22(4):746–757
22. Park SY, Jung DC, Oh YT, et al. (2016) Prostate cancer: pI-RADS version 2 helps preoperatively predict clinically significant cancers. Radiology 280(1):151133
23. Hegde JV, Mulkern RV, Panych LP, et al. (2013) Multiparametric MRI of prostate cancer: an update on state-of-the-art techniques and their performance in detecting and localizing prostate cancer. J Magn Reson Imaging 37(5):1035–1054
24. Hassanzadeh E, Alessandrino F, Olubiyi OI, et al. (2017) Comparison of quantitative apparent diffusion coefficient parameters with prostate imaging reporting and data system V2 assessment for detection of clinically significant peripheral zone prostate cancer. Abdom Radiol (NY) 43(5):1237–12425
25. Fennessy FM, Fedorov A, Penzkofer T, et al. (2015) Quantitative pharmacokinetic analysis of prostate cancer DCE-MRI at 3T: comparison of two arterial input functions on cancer detection with digitized whole mount histopathological validation. Magn Reson Imaging. 33(7):886–894
26. Srigley JR, Humphrey PA, Amin MB, et al. (2009) Protocol for the examination of specimens from patients with carcinoma of the prostate gland. Arch Pathol Lab Med 133(10):1568–1576
27. Buyyounouski MK, Choyke PL, Kattan MW, et al. (2017) Prostate. In: Amin MB, Edge SB, Greene FL, Byrd DR, Brookland RK, Washington MK, et al. (eds) *AJCC Cancer Staging Manual*, 8th edn. New York: Springer, pp 715–726
28. Nowak J, Malzahn U, Baur ADJ, et al. (2014) The value of ADC, T2 signal intensity, and a combination of both parameters to assess Gleason score and primary Gleason grades in patients with known prostate cancer. Acta Radiol 7(1):107–114
29. Jyoti R, Jain TP, Haxhimolla H, Liddell H, Barrett SE (2018) Correlation of apparent diffusion coefficient ratio on 3.0 T MRI with prostate cancer Gleason score. Eur J Radiol Open 5:58–63
30. Lebovici A, Sfrangeu SA, Feier D, et al. (2014) Evaluation of the normal-to-diseased apparent diffusion coefficient ratio as an indicator of prostate cancer aggressiveness. BMC Med Imaging 14:15
31. Itatani R, Namimoto T, Yoshimura A, et al. (2014) Clinical utility of the normalized apparent diffusion coefficient for preoperative evaluation of the aggressiveness of prostate cancer. Jpn J Radiol 32(12):685–691
32. Woo S, Suh CH, Kim SY, Cho JY, Kim SH (2018) Head-to-head comparison between high- and standard-b-value DWI for detecting prostate cancer: a systematic review and meta-analysis. AJR 210(1):91–100
33. Fennessy F, Fedorov A, Vangel M, et al. (2018) Multiparametric MRI as a biomarker of response to neoadjuvant second-generation hormone therapy for localized prostate cancer- a pilot study. Proc Intl Soc Mag Reson Med 2018:26
34. Hurrell SL, McGarry SD, Kaczmarowski A, et al. (2018) Optimized b-value selection for the discrimination of prostate cancer grades, including the cribriform pattern, using diffusion weighted imaging. J Med Imaging (Bellingham) 5(1):011004
35. Feng Z, Min X, Margolis DJA, et al. (2017) Evaluation of different mathematical models and different b-value ranges of diffusion-weighted imaging in peripheral zone prostate cancer detection using b-value up to 4500 s/mm^2. Schwentner C, ed. PLoS ONE 12(2):e0172127
36. Purysko AS, Bittencourt LK, Bullen JA, et al. (2017) Accuracy and interobserver agreement for prostate imaging reporting and data system, version 2, for the characterization of lesions identified on multiparametric MRI of the prostate. AJR 209(2):339–349